Water resource recovery by means of microalgae cultivation in outdoor photobioreactors using the effluent from an anaerobic membrane bioreactor fed with pre-treated sewage

Alexandre Viruela *,[a], Mónica Murgui [b], Tao Gómez-Gil [a], Freddy Durán [a], Ángel Robles [a], María Victoria Ruano [b], José Ferrer [a], Aurora Seco [b]

[a]Instituto de Ingeniería del Agua y Medio Ambiente, IIAMA, Universitat Politècnica de Valencia, Camino de Vera s/n, 46022 Valencia, Spain (e-mail: alvina@upv.es, tagogi@upv.es, fredurpi@upv.es, ngerobma@upv.es, jferrer@hma.upv.es)

[b]Departamentd'Enginyeria Química, EscolaTècnica Superior d'Enginyeria, Universitat de València, Avinguda de la Universitat s/n. 46100 Burjassot, Valencia, Spain (email: monica.murgui@uv.es, m.victoria.ruano@uv.es, aurora.seco@uv.es)

*Corresponding author. Tel. +34 963 877 000 ext. 76176; Fax +34 963 877 618, e-mail address: alvina@upv.es

17   **ABSTRACT**

18   With the aim of assessing the potential of microalgae cultivation for water resource

19   recovery (WRR), the performance of three 0.55 m^3 flat-plate photobioreactors (PBRs)

20   was evaluated in terms of nutrient removal rate (NRR) and biomass production. The

21   PBRs were operated outdoor (at ambient temperature and light intensity) using as

22   growth media the nutrient-rich effluent from an AnMBR fed with pre-treated sewage.

23   Solar irradiance was the most determining factor affecting NRR. Biomass productivity

24   was significantly affected by temperatures below 20 ℃. The maximum biomass

25   productivity (52.3 mg $VSS·L^{-1}·d^{-1}$) and NRR (5.84 mg NH_4-$N·L^{-1}·d^{-1}$ and 0.85 mg PO_4-

26    $P·L^{-1}·d^{-1}$) were achieved at solar irradiance of 395 $\mu E·m^{-2}·s^{-1}$, temperature of 25.5 ℃,

27   and HRT of 8 days. Under these conditions, it was possible to comply with effluent

28   nutrient standards (European Directive 91/271/CEE) when the nutrient content in the

29   influent was in the range of 40-50 mg $N·L^{-1}$ and 6-7 mg $P·L^{-1}$.

30   **Keywords**

31   Flat-plate photobioreactors; microalgae; nutrient removal; outdoor cultivation;

32   wastewater.

33

1. INTRODUCTION

In recent years, there has been an increasing interest in the development of new mainstream (and sidestream) treatment units allowing to move from the current WWTPs towards the so-called water resource recovery facilities (WRRFs). Consequently, maximising energy efficiency and resource recovery has become a key issue in the sewage treatment field (Beuckels et al., 2015).

Microalgae-based systems appear as a "green" alternative for sewage treatment (Judd et al., 2015; Zhou et al., 2014). Autotrophic microalgae are photosynthetic microorganisms that use inorganic carbon (CO_2 and HCO_3^-) for biomass production and obtain the energy needed for growth and metabolism from light. Moreover, the required macronutrients (N and P) are taken up in the form of inorganic compounds such as ammonium (NH_4^+) and phosphate (PO_4^{3-}). The generated algal biomass can be valorised in various ways for energy recovery (biofuel production) and nutrient recovery (fertiliser production) (Brenan and Owende, 2010).

Microalgae cultivation can be applied in different stages of the sewage treatment cycle depending on the wastewater nutrient content (Alcántara et al., 2015; Valverde-Pérez et al., 2015). For instance, Ruiz-Martinez et al. (2012) showed that the effluent from an anaerobic membrane bioreactor (AnMBR) fed with pre-treated sewage can be successfully applied for microalgae cultivation since it is commonly enriched in NH_4^+ and PO_4^{3-}. Therefore, when it is not possible to recycle the effluent from an AnMBR system for irrigation or fertigation purposes, microalgae cultivation represents an interesting alternative for nutrient recovery. In addition, AnMBR have been reported as a promising water resource recovery (WRR) process (see, for instance, Pretel et al., 2016; Smith et al., 2014) since it combines the main advantages of anaerobic-based

58 technology (biogas production and reduced power consumption and sludge production)

59 and filtration-based technology (small footprint, complete retention of biomass and

60 generation of high-quality and solid-free effluent).

61 Hence, the combination of AnMBR and microalgae-based technologies can be

62 considered an interesting approach for recovering nutrients and energy from sewage

63 whilst reducing carbon footprint, providing therefore the desired step from WWTPs to

64 WRRFs.

65 Open pond systems and closed-air photobioreactors (PBRs) are the leading contenders

66 for large-scale microalgae cultivation. Although open ponds present relatively low

67 costs, closed-air PBRs allows efficiently increasing microalgae cultivation yields

68 mainly because these systems reduce culture contamination (e.g. pathogens, predators).

69 Other benefits of closed-air PBRs are: (1) reduced footprint, (2) increased volumetric

70 productivities, (3) enhanced gas (CO_2) transfer, and (4) protection from outdoor

71 climate-related impacts such as rainfall and evaporation (Maity et al., 2014).

72 The application of closed-air PBRs for sewage treatment has been mostly reported at

73 lab-scale using artificial light and/or temperature control (see, for instance, Krustok et

74 al., 2016; Medina and Neis, 2007; Ruiz-Martinez et al., 2012). However, microalgae

75 cultivation in pilot-scale PBRs operated at ambient solar irradiance and temperature has

76 been much less examined (Arbib et al., 2013a; Gouveia et al., 2016), which is necessary

77 for establishing the baselines for future cultivation improvements in this kind of systems

78 (Schoepp et al., 2014).

79 The objective of this study was to evaluate the potential use of microalgae cultivation

80 for nutrient recovery in WRRFs. To this aim, three pilot-scale PBRs (working volume

81 of 0.55 m^3) were operated using the nutrient-rich effluent from an AnMBR pilot-plant

4

82 (Giménez et al., 2011) that treated sewage. Specifically, the AnMBR was fed with

83 effluent from the pre-treatment (screening, degritter and grease removal) of the

84 Carraixet WWTP (Valencia, Spain). The PBR plant was operated outdoor (i.e. at

85 ambient solar irradiance and temperature); and the nutrient loading rate (NLR) varied

86 depending on both Carraixet WWTP intake dynamics and AnMBR performance.

87 Hence, the performance of the PBR system (microalgae growth and nutrient uptake)

88 was evaluated under similar conditions to the ones expected at likely full-scale plants.

89 **2. MATERIALS AND METHODS**

90 **2.1. PBR description**

91 Microalgae cultivation was performed in three outdoor flat-plate PBRs made of

92 transparent methacrylate. Each PBR had a total and working volume of 0.62 m^3 and

93 0.55 m^3, respectively. Their dimensions were 1.25-m height, 2-m width and 0.25-m

94 depth. All three PBRs were south-facing to take full advantage of solar irradiance and

95 were located in the Carraixet WWTP (39º30'04.0''N 0º20'00.1''W, Valencia, Spain).

96 The PBRs were operated independently at different time periods from September to

97 December. Figure 1 shows the flow diagram of the PBR plant used in this study. The

98 plant was fed with the nutrient-rich effluent from an AnMBR pilot plant (see Giménez

99 et al., 2011) that treated sewage. Specifically, the AnMBR was fed with effluent from

100 the pre-treatment (screening, degritter and grease removal) of the Carraixet WWTP

101 (Valencia, Spain). The influent was pumped to a 0.1 m^3 distribution chamber (DC) from

102 which it was fed equally by gravity into three PBRs (PBR1, PBR2 and PBR3).

103 The PBRs were continuously stirred by gas sparging, which promoted proper mixing

104 conditions, avoided wall fouling and ensured adequate CO_2 transference within the

105   broth column. To this aim, one compressor (C) recycled gas continuously from the

106   headspace of the PBRs to the system, which allowed to reduce CO_2 losses as well. The

107   flow-rate of gas entering each PBR was set to 0.061 vvm ($2 \ m^3 \cdot h^{-1}$). To maintain

108   suitable microalgal growth rates and avoid undesirable chemical processes (e.g.

109   phosphate precipitation and free ammonia stripping), pH was controlled at 7.5 by

110   introducing pure CO_2 (99.9%) from a pressurised bottle into the system through the gas

111   recycling pipe. The amount of CO_2 fed to each PBR during the experimental period

112   ranged from 2.45 to 5.73 mg $CO_2 \cdot L^{-1} \cdot d^{-1}$.

113   Each PBR was equipped with a pH-temperature (pHD sc Hach) transmitter and a

114   dissolved oxygen (DO) transmitter (LDO sc Hach). Moreover, an on-line irradiation

115   sensor (Apogee Quantum) was installed on the surface of the PBRs for measuring the

116   photosynthetically active radiation (PAR).

117   **2.2. Microalgae inoculation**

118   Microalgae were originally collected from the secondary settler of the Carraixet

119   WWTP, thus the microorganisms were already adapted to the environmental conditions

120   and sewage matrix. These indigenous microalgae were selected for process inoculation

121   since previous studies shown that a natural bloom of these genus (*Scenedesmus* sp.

122   and/or *Chlorella* sp.) was observed in the reactor when seeking the natural colonisation

123   of the system. Moreover, previous studies conducted with other isolated species resulted

124   in the development of a culture with a vast predomination of *Scenedesmus* sp. and/or

125   *Chlorella* sp. after several days of operation (data not shown).

126   Then, microalgae biomass was pre-cultivated in batch mode at bench-scale using a

127   cylindrical, transparent methacrylate reactor (internal diameter of 20 cm) with a total

128 volume of 10 L. Four arrays of 3 vertical fluorescent lamps (Sylvania Grolux, 18 W),

129 which were distanced each other by 10 cm, illuminated the reactor continuously from a

130 distance of 10 cm. Light intensity was set to 200 $\mu E \cdot m^{-2} \cdot s^{-1}$, measured at the surface of

131 the reactor. This reactor was placed inside a climatic chamber with air temperature

132 control set to 22 ºC. To this aim, effluent from the aforementioned AnMBR was used as

133 growth medium. The biomass in the laboratory reactor formed a stable culture of

134 microalgae with a vast predominance of *Scenedesmus* sp. (>99%). PBR1 was inoculated

135 using microalgae pre-cultivated at laboratory conditions. PBR2 and PBR3 were

136 inoculated using wasted microalgae biomass obtained during the operation of PBR1 and

137 PBR2, respectively. The PBR start-up procedure consisted in the following: i)

138 inoculation of the PBR with the microalgae culture from laboratory or a previously

139 operated PBR (10% of total working volume with volatile suspended solids (VSS)

140 concentration between 300-500 $mg \cdot L^{-1}$); ii) conditioning stage in batch mode until

141 reaching pseudo-steady state conditions (i.e. reaching stable VSS concentration); and

142 iii) start-up of an automatic semi-continuous feeding mode during daylight hours.

143 **2.3. PBR operation**

144 As reported before, the PBRs were fed using the nutrient-rich effluent from an AnMBR

145 fed with pre-treated sewage. Therefore, the nutrient load entering the PBRs varied

146 depending on both WWTP intake dynamics and AnMBR performance. The main

147 characteristics of the influent to the PBR plant during the whole experimental period

148 were ammonium (NH_4^+) of 55.2 ± 15.6 mg N·L^{-1}, phosphate (PO_4^{3-}) of 6.8 ± 1.7 mg

149 P·L^{-1}, N:P mass ratio of 8.1 ± 0.7 g N·g^{-1}P, total COD of 35 ± 6, alkalinity of 448 ± 96

150 mg CaCO$_3$·L^{-1} and VFA of 1.75 ± 0.5 mg HAc·L^{-1}. Nitrite (NO_2^-) and nitrate (NO_3^-) in

151 the influent were negligible.

152 The whole experimental period (from September to December) was divided into

153 different operating periods (i, ii and iii) according to the operated PBR. Specifically,

154 period i, ii and iii comprised the operation of PBR1, PBR2 and PBR3, respectively. The

155 PBRs were operated within September-December, October-November and October-

156 December, respectively. In addition, operating period i and iii were sub-divided into two

157 sub-periods (sub-periods i1 and i2 and sub-periods iii1 and iii2) according to the

158 operating HRT and environmental conditions, respectively. Table 1 shows the average

159 operating and environmental conditions for the pseudo-steady state reached at the end of

160 each operating (sub-)period. Temperature and solar irradiation varied depending on

161 ambient conditions. Two HRTs were evaluated in this study: 14 and 8 days. HRT of 14

162 days was only applied during sub-period i2.

163 Allylthiourea was used in order to inhibit nitrification in the PBRs (Krustok et al.,

164 2016). Thus, the main process responsible for nitrogen depletion was nitrogen uptake by

165 microalgae. Allylthiourea was added at the concentration of 5 or 10 $mg \cdot L^{-1}$.

166 In this study, biomass productivity (mg $VSS \cdot L^{-1} \cdot day^{-1}$) and nitrogen-NRR (mg $N \cdot L^{-1} \cdot day^{-1}$)

167 $^{-1} \cdot day^{-1}$) and phosphorus-NRR (mg $P \cdot L^{-1} \cdot day^{-1}$) were calculated as follows:

168 Biomass productivity $= \frac{X_{VSS}}{HRT}$ (Eq. 1)

169 where X_{VSS} (mg $VSS \cdot L^{-1}$) is the volatile suspended solids concentration in the PBR.

170 nitrogen $-$ NRR $= \frac{N_i - N_e}{t \cdot V_{PBR}}$ (Eq. 2)

171 where N_i is the mass of nitrogen entering the system, N_e is the mass of nitrogen leaving

172 the system in the effluent, t is the interval of time considered, and V_{PBR} is the volume of

173 the medium in the PBR.

174     $\text{phosphorus} - \text{NRR} = \frac{P_i - P_e}{t \cdot V_{PBR}}$ (Eq. 3)

175   where P_i is the average mass of phosphorus entering the system and P_e is the average

176   mass of phosphorus leaving the system in the effluent.

2.4. Sampling and Analytical Methods

178   In order to evaluate the process performance, grab samples were collected from influent

179   and effluent streams three times per week. It is important to note that the PBRs were

180   operated semi-continuously at large HRTs (14 and 8 days). Therefore, the system

181   equalised possible sudden variations in the influent load. Moreover, the influent to the

182   PBR plant was the effluent from an AnMBR system operated at HRT of around 1 day

183   and SRT of 70 days. Thus, grab samples allowed capturing the dynamics observed in

184   influent and effluent streams of the PBRs. The soluble fraction (filtrate) was obtained

185   by vacuum filtration with 0.45 mm pore size filters (Millipore). Ammonium (NH_4^+),

186   nitrite (NO_2^-), nitrate (NO_3^-), and phosphate (PO_4^{3-}) were determined in the filtrate

187   according to Standard Methods (APHA, 2005) (methods 4500-NH3-G, 4500-NO2-B,

188   4500-NO3-H, and 4500-P-F, respectively) in a Smartchem 200 automatic analyser

189   (Westco Scientific Instruments, Westco). Effluent VSS was also analysed according to

190   Standard Methods (APHA, 2005) (method 2540 E). All measurements were performed

191   in duplicate. The uncertainty associated with each presented value includes: 1) the

192   standard deviation of duplicates analysed throughout the experimental period, and 2) the

193   coefficient of variation associated with the analytical method.

194   Eukaryotic cell number (cells·L^{-1}) was determined by epifluorescence microscopic

195   methods (Pachés et al., 2012) using a Leica DM2500 microscope which incorporates a

196   100x oil-immersion objective. In this measurement, a minimum of 300 cells were

197   counted and at least 100 cells of the most abundant species were counted with an error

198   below 20% (Lund et al., 1958).

199   **2.5. Partial least squares regression (PLSR)**

200   Partial least squares regression (PLSR) is a type of multivariate analysis (two-block

201   predictive PLS) for relating two data matrices, X and Y, by a linear multivariate model

202   (Wold et al., 2001). PLSR allows to model one or several responses (Y) from a set of

203   predictors (X) while reducing the dimensionality of the explanatory variables.

204   Moreover, this method identifies the predictors that better explain the information

205   content between the X and Y data sets.

206   mixOmics library (http://www.mixOmics.org) through the R statistical package version

207   3.2.3 (http://www.R-project.org) was used in this study to implement the PLSR

208   algorithm.

209   PLSR algorithm was conducted to evaluate the effect of different operating and

210   environmental factors (i.e. predictors, X) on several process performance indicators (i.e.

211   responses, Y). Specifically, the set of predictors evaluated consisted of the following:

212   nitrogen to phosphorus ratio in the influent, nutrient loading rate referred to nitrogen,

213   nutrient loading rate referred to phosphorus, temperature and light intensity. The

214   responses evaluated consisted of: biomass productivity, nutrient removal rate referred to

215   nitrogen and nutrient removal rate referred to phosphorus.

216   **3. RESULTS AND DISCUSSION**

217   By way of example, Figure 2 illustrates the time evolution profiles of PAR, pH, DO and

218   temperature within two days of operation of period ii. These time evolution profiles

219   followed a similar pattern in the rest of operating periods evaluated. As this figure

220   shows, DO behaved similarly to PAR during daylight hours, recording therefore

221   maximum DO values around midday. Despite oxygen consumption due to microalgae

222   respiration, an upward trend was observed in DO during night-time hours. This upward

223   trend was related to temperature variations affecting oxygen solubility in water. Indeed,

224   DO varied according to culture temperature during night-time hours, meeting the

225   saturation concentration of DO in water for each operating temperature.

226   CO_2 was automatically fed to the system in order to keep the pH at values around 7.5,

227   even during daylight hours with high solar irradiance. It has been extensively reported

228   that pH values above 9 negatively affect microalgae culture since it allows phosphate

229   precipitation and free ammonia volatilisation (Arbib et al., 2013b).

230   During the whole experimental period (periods i, ii and iii), the PBRs resulted in a

231   stable culture of microalgae with a vast predominance of *Scenedesmus* sp. (> 99%) and

232   one-time appearances of *Chlorella* sp. Those microalgae species (*Scenedesmus* sp. and

233   *Chlorella* sp.) are the species most frequently observed in microalgae-based wastewater

234   treatment systems (Morales-Amaral et al., 2015). By way of example, Figure A.1 in

235   Appendix A shows a microscopic image of the microalgae culture from PBR1.

236   The predominance of a given species of microalgae among others seems to be related

237   not only to environmental conditions such as temperature and solar irradiance intensity

238   but also to the availability of N and P in the medium since microalgae are able to adjust

239   their intracellular macronutrient content (Beuckels et al., 2015). Rhee (1978) found that

240   the optimal cellular N:P mass ratio of *Scenedesmus* sp. was 13.6 g $N \cdot g^{-1}$ P. Silva et al.

241   (2015) reported an optimal N:P mass ratio of 3.6 for *Chlorella* sp. In our study, the

242   observed influent N:P mass ratio was 8.1 ± 0.7, which favoured the predominance of

243 *Scenedesmus* sp. versus *Chlorella* sp. In addition, the influent N:P mass ratio was in the

244 optimum range for nutrient removal reported by Xin et al. (2010) for *Scenedesmus* sp.

245 (5-20 g N·g^{-1} P). In addition, there are other factors, such as environmental conditions

246 (temperature and solar irradiance), pH, nutrient levels, shear stress due to aeration

247 intensity, among others, that also affect the inter-specie competition and therefore the

248 prevailing species.

249 As regards organic matter removal, the influent to the PBRs was characterised by low

250 COD levels (35 ± 6 mg/L). Most of this COD was non-biodegradable as this stream

251 came from an AnMBR plant that degraded almost all biodegradable organic matter.

252 Indeed, soluble COD concentrations in influent and effluent streams from the PBRs

253 were nearby the same, which corroborated that there was not meaningful heterotrophic

254 activity (either bacteria or microalgae) throughout the experimental period.

255 **3.1. Period i. PBR performance at different levels of temperature and HRT**

256 As Figure 3 shows, PBR1 was operated for 94 days at different levels of temperature

257 (around 25 and 15 ºC for the pseudo-steady state reached at the end of sub-periods i1

258 and i2, respectively – see Table 1) and HRT (8 during sub-period i1 and 14 days during

259 sub-period i2). As previously commented, period i was divided into two sub-periods

260 according to the applied HRT. Although both solar irradiance and temperature varied

261 freely depending on ambient conditions due to the outdoor operation, PAR resulted in

262 similar average levels for the pseudo-steady state reached at the end of sub-periods i1

263 and i2 (see Table 1). Therefore, its effect on average process performance was not

264 strictly considered during operating period i.

265 On the other hand, the ammonium and phosphate contents in the influent remained

266 fairly constant until day 60 (see Figure 3a). After day 60 of operation, these contents

267 underwent an important increase according to WWTP intake dynamics and AnMBR

268 operation, reaching average pseudo-steady state values at the end of the operating

269 period of 84.6 mg NH_4-$N\cdot L^{-1}$ and 9.7 mg PO_4-$P\cdot L^{-1}$. Nevertheless, NLR remained in

270 similar values at the end of sub-periods i1 and i2 (see Table 2) because of operating at

271 different HRT levels.

272 As Figure 3a shows, the effluent ammonium and phosphate concentrations increased

273 during sub-period i1 (operating at HRT of 8 days) until reaching the pseudo-steady state

274 around day 24. Although temperature remained close to the optimum value for

275 *Scenedesmus* sp. (optimal growth rates were reported by Xin et al. (2011) at 25 ºC), the

276 low values recorded in solar irradiance (average pseudo-steady state value of 148 ± 36

277 $\mu E \cdot m^{-2} \cdot s^{-1}$) combined with the applied HRT favoured biomass washout. Specifically,

278 biomass concentration decrease from approx. 300 mg $VSS\cdot L^{-1}$ and $5 \cdot 10^9$ $cells\cdot L^{-1}$ to

279 values of around 200 mg $VSS\cdot L^{-1}$ and $3 \cdot 10^9$ $cells\cdot L^{-1}$ at the end of sub-period i1.

280 Specifically, the pseudo-steady state biomass productivity and nutrient removal rate

281 (NRR) in sub-period i1 resulted in 23.4 ± 0.6 mg $VSS\cdot L^{-1}\cdot d^{-1}$ and 2.08 ± 1.17 mg NH_4-

282 $N\cdot L^{-1}\cdot d^{-1}$ and 0.17 ± 0.17 mg PO_4-$P\cdot L^{-1}\cdot d^{-1}$, respectively; whilst the pseudo-steady state

283 ammonium and phosphate removal efficiency resulted in 41.6 ± 4.0 % and $36.1 \pm$

284 5.9 %, respectively.

285 HRT was increased from 8 to 14 days at the very beginning of sub-period i2. From day

286 30 to 60, the increment in HRT resulted in a consequent decrease in NLR since the

287 influent ammonium and phosphate concentrations remained nearby constant (see Figure

288 3a). In addition to the increment in HRT, an increase in solar irradiance was also

289 registered between days 30 and 60. Due to the increase registered in both HRT and

13

290 PAR, nitrogen-NRR and biomass productivity experimented a significant increase.

291 Specifically, nitrogen-NRR increased from approx. 1.25 to 2.35 mg NH_4-$N \cdot L^{-1} \cdot d^{-1}$ and

292 biomass concentration increased from approx. 176 to 361 $mg \cdot L^{-1}$. This was mainly

293 related to reduced microalgae washout and increased microalgae growth rate due to

294 increased HRT and PAR, respectively.

295 However, the increment in HRT was compensated at the end of sub-period i2 by the

296 increased recorded in the influent ammonium and phosphate concentrations from day 60

297 until the end of the operating period (see Figure 3a). Indeed, NLR and N:P ratios

298 yielded values comparable to the ones recorded during the pseudo-steady state of sub-

299 period i1 (see Table 1). Moreover, after day 52, the daily average temperature

300 experimented an important decrease, remaining in values around 15 ºC until the end of

301 sub-period i2. This values were far away from the optimal temperature of 25 ºC

302 reported by Xin et al. (2011). On the other hand, the solar irradiance reached values at

303 the end of sub-period i2 similar to the ones from the pseudo-steady state from sub-

304 period i1 (see Table 1). Under those environmental and operating conditions, PBR1

305 achieved similar biomass concentrations at the end of sub-period i2 (around 200 mg

306 $VSS \cdot L^{-1}$ and $3 \cdot 10^9$ $cells \cdot L^{-1}$) than the ones obtained at the end of sub-period i1.

307 Nevertheless, biomass productivity (13.8 ± 1.1 mg $VSS \cdot L^{-1} \cdot d^{-1}$) and nitrogen-NRR

308 (0.81 ± 0.52 mg NH_4-$N \cdot L^{-1} \cdot d^{-1}$) were lower. Hence, the results showed that nearly

309 doubling HRT does not guarantee increased biomass productivity and NRR in outdoor

310 microalgae cultivation when operating at low temperature (around 15 ºC). In this

311 respect, Larsdotter (2006) stated that HRT must not exceed the required time to

312 maintain optimum growth rates of microalgae. Indeed, Kim et al. (2014) concluded that

313 increasing HRT excessively may result in low NRR and biomass productivity. Thus, it

314 is necessary to optimise the operating HRT depending on environmental conditions.

315　Allylthiourea concentration in PBR1 was set to 5 mg·L^{-1} during sub-period i1, which

316　seemed to be enough to control nitrifying bacteria since nitrite and nitrate

317　concentrations remained close to 0 mg N·L^{-1}. However, an important nitrifying activity

318　was registered between days 45 and 50 (see Figure 3a), which was mainly attributed to

319　the increase in HRT. Therefore, in order to inhibit ammonium oxidation bacteria and to

320　study the potential microalgae nutrient uptake, allylthiourea concentration was increased

321　from 5 to 10 mg·L^{-1} for the rest of the experimental period (nitrite and nitrate

322　concentrations quickly decreased according to the dilution rate).

323　The microalgae ammonium-NRR observed throughout operating period i was lower

324　than other values reported in literature for *Scenedesmus* sp. For instance, Park et al.

325　(2010) reported NRR of 5-6 mg NH$_4$-N·L^{-1}·d^{-1} when treating the nutrient-rich effluent

326　from an anaerobic digester fed with piggery wastewater and applying cycles of artificial

327　light (PAR of 200 µE·m^{-2}·s^{-1} during 12 hours per day). On the other hand, Ruiz-

328　Martinez et al. (2012) reported NRR of 19.5 mg NH$_4$-N·L^{-1}·d^{-1} and 3.7 mg PO$_4$-P·L^{-1}·d^{-}

329　^{1} treating effluent from the AnMBR used in this study and working at lab-scale with

330　continuous artificial illumination (PAR of 114 and 198 µE·m^{-2}·s^{-1} during 24 hours per

331　day). These results suggest that higher NRR could be obtained under more favourable

332　outdoor conditions.

333　As Figure 3a shows, within operating period i, the higher the influent nutrient

334　concentration the higher the effluent nutrient concentration. This behaviour is in

335　agreement with Arbib et al. (2013a), who reported that effluent nutrient concentration

336　trends follow influent nutrient concentration trends in non-nutrient limited and outdoor

337　microalgae cultivation (limited by ambient temperature and light conditions), for given

338　operating conditions.

3.2. Period ii. PBR performance at nearby stable levels of solar irradiance and temperature

As Figure 4 shows, PBR2 was operated for 27 days at HRT of 8 days and fairly constant NLR (47.0 ± 2.6 mg NH_4-N·L^{-1} and 5.8 ± 0.8 mg PO_4-P·L^{-1}). During this operating period, solar irradiance and temperature varied freely depending on ambient conditions as well. Nonetheless, PAR and temperature remained nearby stable around a given level (see Table 1).

Biomass productivity and NRR remained fairly constant during the whole operating period, resulting in values of 30.5 ± 1.8 mg VSS· L^{-1}·d^{-1} and 3.94 ± 0.44 mg NH_4-N·L^{-1}·d^{-1} (ammonium removal efficiency of 54.4 ± 4.0 %) and 0.41 ± 0.07 mg PO_4-P· L^{-1}·d^{-1} (phosphorus removal efficiency of 55.9 ± 0.9 %), respectively, within the pseudo-steady state period. Although average operating temperature and NLR during period ii were similar to the ones from sub-period i1 (also operated at HRT of 8 days), period ii resulted in higher NRR and biomass productivity. Microalgae concentration yielded values of around 250 mg VSS·L^{-1} and $5·10^9$ cells·L^{-1} at the end of operating period ii (these values were also higher than the ones resulting from sub-period i1). The higher NRR and biomass productivity obtained in period ii was attributed to the higher solar irradiance achieved at the pseudo-steady state and also to the fact that no cloudy days were registered during period ii (cloudy day was defined as days with average PAR below 125 $\mu E·m^{-2}·s^{-1}$).

3.3. Period iii. PBR performance at different levels of NLR and solar irradiance

As Figure 5 shows, PBR3 was operated for 64 days at different levels of solar irradiance (around 402 and 290 $\mu E \cdot m^{-2} \cdot s^{-1}$) and NLR (2.61 g NH_4-N·d^{-1} and 0.34 g PO_4-N·d^{-1}, and 5.00 g NH_4-N·d^{-1} and 0.58 g PO_4-N·d^{-1}) at the pseudo-steady state reached at the end of sub-periods iii1 and iii2, respectively (see Table 1). Although temperature varied freely depending on ambient conditions, it resulted in similar levels for both pseudo-steady states (see Table 1). Thus, its effect on average process performance was not strictly considered during operating period iii. However, a significant decrease in temperature was observed throughout sub-period iii1, registering daily average values around 30 ºC at the beginning and 20 ºC at the end of this sub-period.

Equal to PBR1 (operating period i), the ammonium and phosphate contents in the influent to PBR3 remained fairly constant during sub-period iii1 (47.2 ± 2.9 mg NH_4-N·L^{-1} and 6.1 ± 0.7 mg PO_4-P·L^{-1}, see Figure 5a). Nevertheless, these contents suffered an important increase according to WWTP intake dynamics and AnMBR operation during sub-period iii2, reaching average pseudo-steady state values at the end of the operating period of 84.6 mg NH_4-N·L^{-1} and 9.7 mg PO_4-P·L^{-1}. Contrary to operating period i, NLR increased significantly from sub-period iii1 to sub-period iii2 (see Table 1) due to operating at constant HRT levels.

Sub-period iii1 resulted in pseudo-steady state NRR values of 4.75 ± 0.03 mg NH_4-N·L^{-1}·d^{-1} (removal efficiency of 75.2 ± 2.2 %) and 0.51 ± 0.08 mg PO_4-P·L^{-1}·d^{-1} (removal efficiency of 77.9 ± 1.4 %). Moreover, this sub-period resulted in the maximum gross NRR of the study: 5.84 mg NH_4-N·L^{-1}·d^{-1} and 0.85 mg PO_4-P·L^{-1}·d^{-1}, which corresponded to removal efficiencies of 84.1% and 95.1% for N and P, respectively.

383　However, a significant decrease in NRR was observed in sub-period iii2, with minimum

384　average values of 1.99 mg NH_4-$N \cdot L^{-1} \cdot d^{-1}$ and 0.30 mg PO_4-$P \cdot L^{-1} \cdot d^{-1}$ at the end of the

385　sub-period (ammonium and phosphorus removal efficiencies of 69.4% and 66.2%,

386　respectively).The pseudo-steady state NRR values of sub-period iii2 were 3.35 ± 0.57

387　mg NH_4-$N \cdot L^{-1} \cdot d^{-1}$ (removal efficiency of 36.3 ± 6.5 %) and 0.61 ± 0.13 mg PO_4-$P \cdot L^{-1}$

388　$^{-1} \cdot d^{-1}$ (removal efficiency of 45.5 ± 5.3 %).

389　Similar to the performance of PBR1, Figure 5 illustrates how the higher the influent

390　nutrient concentration is the higher the effluent nutrient concentration is in non-nutrient

391　limited conditions for microalgae cultivation operated at given conditions (see sub-

392　periods i2 and iii2). On the other hand, in the case of sub-period iii1 (PBR3

393　performance), N and P were removed by *Scenedesmus* sp. below the current EU

394　emission standards (10 mg $N \cdot L^{-1}$ and 2 mg $P \cdot L^{-1}$, 91/271/CEE and 98/15/EC Urban

395　Wastewater Treatment Directive, European Commission Directive, 1998) when the

396　influent nutrient content was around 40-50 mg $N \cdot L^{-1}$ and 6-7 mg $P \cdot L^{-1}$. These results are

397　in agreement with Beuckels et al. (2015), who operated at bench-scale and optimal

398　temperature and light.

399　Concerning the pseudo-steady state biomass productivity, maximum values of around

400　41.0 ± 2.0 mg $VSS \cdot L^{-1} \cdot d^{-1}$ were achieved during sub-period iii1. However, these values

401　decreased as the temperature and solar irradiance declined throughout operating period

402　iii (see Figure 5b). Indeed, the pseudo-steady state biomass productivity decreased until

403　33.9 ± 3.1 mg $VSS \cdot L^{-1} \cdot d^{-1}$ in sub-period iii2. The pseudo-steady state VSS and cellular

404　density values decreased from 432 to 242 mg $VSS \cdot L^{-1}$ and from $9.2 \cdot 10^9$ to $1.78 \cdot 10^9$

405　$cells \cdot L^{-1}$. The significant decrease observed in total cells compared to VSS

406　concentration was attributed to an increase in the ratio of dead organic matter to

407 microalgae, which was promoted by reduced daily average temperature and solar

408 irradiance.

3.4. Microalgae productivity and NRR in outdoor PBRs

410 Table 2 summarises the average values of the main process performance indicators

411 related to nutrient uptake and microalgae growth calculated within the pseudo-steady

412 state of each operating (sub-)period. As previously commented, these pseudo-steady

413 results were obtained when nearby stable VSS were achieved after having operated for a

414 minimum time period of three cycles of HRT.

415 As commented before, sub-period iii1 resulted in the maximum NRR and biomass

416 productivity revealed in this study (52.3 mg VSS$\cdot$L$^{-1}\cdot$d^{-1}, and 5.84 mg NH$_4$-N$\cdot$L$^{-1}\cdot$d^{-1}

417 and 0.85 mg PO$_4$-P$\cdot$L$^{-1}\cdot$d^{-1}, respectively). This sub-period was operated at 8 days of

418 HRT and favourable environmental conditions: influent nutrient content was around 40-

419 50 mg N$\cdot$L^{-1} and 6-7 mg P$\cdot$L^{-1}, solar irradiance of around 402 μE$\cdot$m$^{-2}\cdot$s^{-1}, and

420 temperature of about 21 ºC. Moreover, the environmental and operating conditions

421 within sub-period iii1 allowed to meet effluent nutrient standards (7.2 $\pm$ 3.9 mg NH$_4$-

422 N$\cdot$L^{-1} and 0.6 $\pm$ 0.4 mg PO$_4$-P$\cdot$L^{-1}) legislated by the European Directive 91/271/CEE.

423 It is worth noting the direct effect that temperature and light intensity has on microalgae

424 cultivation. Indeed, steady state conditions are rarely achieved due to the significant

425 dynamics on ambient light intensity and temperature when operating outdoor. By way

426 of example, Figure 6 illustrates the evolution during operating period iii of: (a) NRR

427 and solar irradiance and temperature, and (b) biomass productivity and solar irradiance

428 and temperature. This figure shows how NRR and biomass productivity followed a

429 similar pattern to both solar irradiance and temperature. Solar irradiance was identified

430   as a key factor affecting NRR in the short-term, whilst temperature was found to have a

431   direct impact on biomass productivity. These observations were corroborated by means

432   of PLSR algorithm (see Figure A.2 in Appendix A). Biomass productivity was directly

433   affected by temperature, while N-NRR was directly correlated with light intensity. On

434   the other hand, N-NRR was inversely correlated with N-NLR. Nevertheless, in this

435   case, N-NLR increased within sub-period iii2 whilst light intensity and temperature

436   decreased, overlapping therefore the individual effect of both NLR and environmental

437   conditions on NRR. As regards P-NRR, it was observed that one key factor affecting P-

438   NRR was the nitrogen to phosphorus ratio in the influent. Specifically, P-NRR was

439   inversely affected by this ratio, indicating that the higher the phosphorus content in the

440   influent is, the higher the P-NRR achieved (within the operating conditions evaluated in

441   this study). Nonetheless, further data from long-term operation should be necessary to

442   obtain more accurate statistical correlations.

443   Further research is needed in order to accurately determine the optimum combination of

444   environmental and operating conditions resulting in enhanced NRR and biomass

445   productivity. In this study, biomass productivity was around the lower bound for

446   *Scenedesmus* sp. (30-260 mg·L^{-1}·d^{-1}) (Mata et al., 2010). Thus, the results obtained in

447   this study are lower than the ones obtained, for instance, at bench-scale. Nevertheless, it

448   is important to note that other authors (e.g. Van Den Hende et al., 2014) also reported

449   an important decrease in NRR when scaling-up microalgae cultivation processes from

450   lab- to pilot-scale. This decreased process yield could be related to one of the most

451   detrimental limitations of continuously-operated PBRs, which is the biomass washout

452   problem (Bilad et al., 2014). Biomass productivity could be improved decoupling

453   biomass retention time (BRT) and HRT in a membrane photobioreactor (MPBR).

454   Membrane filtration would provide complete retention of biomass, preventing biomass

455   washout thus allowing to increase both biomass concentration and productivity

456   (Marbelia et al., 2014).

457   **4. CONCLUSIONS**

458   Outdoor experiments in pilot-scale, closed-air PBRs reflected the significant impact of

459   environmental conditions (i.e. temperature and solar irradiance) on microalgae

460   cultivation for WRR. Temperatures below 20 ºC significantly affected biomass

461   productivity. Solar irradiance was a key factor affecting NRR in the short-term. Nutrient

462   concentration met effluent standards (European Directive 91/271/CEE) when operating

463   at favourable environmental conditions. Overall, NRR and biomass productivity should

464   be further improved. Optimum combinations of operating and environmental conditions

465   need to be obtained. Since the washout of biomass is a key limiting factor, the

466   combination of microalgae cultivation and membrane filtration would enhance the

467   process performance.

468

469   **Appendix A**

470   Supplementary material.

471

REFERENCES

1. Alcántara, C., Domínguez, J.M., García, D., Blanco, S., Péreza, R., García-Encina, P.A., Muñoz, R., 2015. Evaluation of wastewater treatment in a novel anoxic–aerobic algal–bacterial photobioreactor with biomass recycling through carbon and nitrogen mass balances. Bioresour. Technol. 191, 173-186.

2. APHA, 2005. Standard methods for the examination of water and wastewater, 20th ed., American Public Health Association, Washington, DC.

3. Arbib, Z., Ruiz, J., Álvarez-Díaz, P., Garrido-Pérez, C., Barragan, J.,Perales, J.A., 2013a. Long term outdoor operation of a tubular airlift pilot photobioreactor and a high rate algal pond as tertiary treatment of urban wastewater. Ecol. Eng. 52, 143-153.

4. Arbib, Z., Ruiz, J., Álvarez-Díaz, P., Garrido-Pérez, C., Barragan, J., Perales, J.A., 2013b. Effect of pH control by means of flue gas addition on three different photo-bioreactors treating urban wastewater in long-term operation. Ecol. Eng. 57, 226-235.

5. Beuckels, A., Smolders, E., Muylaert, K., 2015. Nitrogen availability influences phosphorus removal in microalgae-based wastewater treatment. Water Res. 77, 98-106.

6. Bilad, M.R., Discart, V., Vandamme, D., Foubert, I., Muylaert, K., Vankelecom, F.J., 2014. Coupled cultivation and pre-harvesting of microalgae in a membrane photobioreactor (MPBR). Bioresour. Technol. 155, 410–417.

7. Brenan, M., Owende, P., 2010. Biofuels from microalgae – A review of technologies for production, processing, and extraction of biofuels and co-products. Renew. Sust. Energ. Rev. 14, 557–577.

503   8.   Giménez, J.B., Robles, A., Carretero, L., Duran, F., Ruano, M.V., Gatti, M.N.,

504   Ribes, J., Ferrer, J., Seco, A., 2011. Experimental study of the anaerobic urban

505   wastewater treatment in a submerged hollow-fiber membrane bioreactor at pilot scale.

506   Bioresour. Technol. 102, 8799-8806.

507   9.   Gouveia, L., Graça, S., Sousa, C., Ambrosano, L., Ribeiro, B., Botrel, E.P.,

508   Castro Neto, P., Ferreira, A.F., Silva, C.M., 2016. Microalgae biomass production

509   using wastewater: Treatment and costs Scale-up considerations. Algal Res. 16, 167-

510   176.

511   10.   Judd, S., van den Broecke, L.J.P., Shurair, M., Kuti, Y., Znad, H., 2015. Algal

512   remediation of CO_2 and nutrient discharges: A review. Water Res. 87, 356-366.

513   11.   Kim, B-H, Kang, Z., Ramanan, R., Choi, J-E., Cho, D-H., Oh, H-M., Kim, H-S.,

514   2014. Nutrient removal and biofuel production in high rate algal pond using real

515   municipal wastewater. J. Microbiol. Biotechn. 24, 1123-1132.

516   12.   Krustok, I., Odlare, M., Truu, J., Nehrenheim, E., 2016. Inhibition of

517   nitrification in municipal wastewater-treating photobioreactors: Effect on algal growth

518   and nutrient uptake. Bioresour. Technol. 202, 238-243.

519   13.   Larsdotter, K., 2006. Wastewater treatment with microalgae – a literature

520   review. Vatten 62, 31-38.

521   14.   Lund, J.W.G., Kipling, C., Le Cren, E.D., 1958. The inverted microscope

522   method of estimating algal numbers and the statistical basis of estimations by

523   counting, Hydrobiologia 11, 143-170.

524   15.   Marbelia, L., Bilad, M.R., Passaris, I., Discart, V., Vandamme, D., Beuckels, A.,

525   Muylaert, K., Vankelecom, Ivo F.J., 2014. Membrane photobioreactors for integrated

526   microalgae cultivation and nutrient remediation of membrane bioreactors effluent.

527   Bioresour. Technol. 163, 228-235.

528   16.   Mata, T., Martins, A.A., Caetano, N.S., 2010. Microalgae for biodiesel

529   production and other applications: a review. Renew. Sust. Energ. Rev. 14, 217-232.

530   17.   Maity J.P., Bundschuh J., Chen C-Y., Bhattacharya, P., 2014. Microalgae for

531   third generation biofuel production, mitigation of greenhouse gas emissions and

532   wastewater treatment: Present and future perspectives – A mini review. Energy 78,

533   104-113.

534   18.   Medina, M., Neis, U., 2007. Symbiotic algal bacterial wastewater treatment:

535   Effect of food to microorganism ratio and hydraulic retention time on the process

536   performance. Water Sci. Technol. 55,165-171.

537   19.   Morales-Amaral, M.M., Gómez, C., Acién, F.G., Fernández-Sevilla, J.M.,

538   Molina-Grima, E., 2015. Production of microalgae using centrate from anaerobic

539   digestion as the nutrient source. Algal Res. 9, 297-305.

540   20.   Pachés, M., Romero, I., Hermosilla, Z., Martinez-Guijarro, R., 2012. PHYMED:

541   An ecological classification system for the Water Framework Directive based on

542   phytoplankton community composition. Ecol. Indic. 19, 15-23.

543   21.   Park, J., Jin, H., Lim, B.-R., Park, K.-Y., Lee, K., 2010. Ammonia removal from

544   anaerobic digestion effluent of livestock waste using green alga *Scenedesmus* sp.

545   Bioresour. Technol. 101, 8649-8657.

546   22.   Pretel, R., Robles, A., Ruano, M.V., Seco, A., Ferrer, J., 2016. Economic and

547   environmental sustainability of submerged anaerobic MBR-based (AnMBR-based)

548   technology as compared to aerobic-based technologies for moderate-/high-loaded

549   urban wastewater treatment. J. Environ. Manage. 166, 45-54.

550   23.   Rhee, G.Y., 1978. Effects of N:P atomic ratios and nitrate limitation on algal

551   growth, cell composition, and nitrate uptake. Limnol. Oceanogr. 23, 10-25.

552   24.   Ruiz-Martinez, A., Martin Garcia, N., Romero, I., Seco, A., Ferrer, J., 2012.

553   Microalgae cultivation in wastewater: Nutrient removal from anaerobic membrane

554   bioreactor effluent. Bioresour. Technol. 126, 247-253.

555   25.   Schoepp, N.G., Stewart, R.L., Sun, V., Quigley, A.J., Mendola, D., Mayfield,

556   S.P., Burkart, M.D., 2014. System and method for research-scale outdoor production

557   of microalgae and cyanobacteria. Bioresour. Technol. 166, 273-281.

558   26.   Silva, N.F.P., Gonçalves, A.L., Moreira, F.C., Silva, T.F.C.V., Martins, F.G.,

559   Alvim-Ferraz, M.C.M., Boaventura, R.A.R., Vilar, V.J.P., Pires, J.C.M., 2015.

560   Towards sustainable microalgal biomass production by phycoremediation of a

561   synthetic wastewater: A kinetic study. Algal Res. 11, 350-358.

562   27.   Smith, A.L., Stadler, L.B., Cao, L., Love, N.G., Raskin, L., Skerlos, S.J., 2014.

563   Navigating wastewater energy recovery strategies: A life cycle comparison of

564   anaerobic membrane bioreactor and conventional treatment systems with anaerobic

565   digestion. Environ. Sci. Technol. 48, 5972-5981.

566   28.   Valverde-Pérez, B., Ramin, E., Smets, B.F., Plósz, B.G., 2015. EBP2R – An

567   innovative enhanced biological nutrient recovery activated sludge system to produce

568   growth medium for green microalgae cultivation. Water Res.68, 821-830.

569   29.   Van Den Hende, S., Beelen, V., Bore, G., Boon, N., Vervaeren, H., 2014.Up-

570   scaling aquaculture wastewater treatment by microalgal bacterial flocs: From lab

571   reactors to an outdoor raceway pond. Bioresour. Technol. 159, 342-354.

572   30.   Wold, S., Sjöström, M., Eriksson, L., 2001. PLS-regression: a basic tool of

573   chemometrics. Chemom. Intell. Lab. Syst. 58, 109–130.

574   31.   Xin, L., Hong-Ying, H. Ke, G., Ying-xue, Z., 2010. Effects of different nitrogen

575   and phosphorus concentrations on the growth, nutrient uptake, and lipid accumulation

576   of a freshwater microalga *Scenedesmus* sp. Bioresour. Technol. 101, 5494-5500.

577   32.   Xin, L., Hong-Ying, H., Yu-ping, Z., 2011. Growth and lipid accumulation

578   properties of a freshwater microalga *Scenedesmus* sp. under different cultivation

579   temperature. Bioresour. Technol. 102, 3098-3102.

580   33.   Zhou, W., Chen, P., Min, M., Ma, X., Wang, J., Griffith, R., Hussain, F., Peng,

581   P., Xie, Q., Li, Y., Shi, J., Meng, J., Ruan, R., 2014. Environment-enhancing algal

582   biofuel production using wastewaters. Renew. Sust. Energ. Rev. 36, 256-269.

583

TABLE AND FIGURE CAPTIONS

**Table 1:** Average operating and environmental conditions within the pseudo-steady state of each operating (sub-)period.

Table 2: NRR, nutrient removal efficiency and biomass productivity within the pseudo-steady state of each operating (sub-)period.

Figure 1: Flow diagram of the PBR system. Nomenclature: DC: distribution chamber; PBR: photobioreactor; P: pump; C: compressor.

Figure 2: Time evolution profiles within two days of operation of solar irradiance (PAR), temperature, pH and DO.

Figure 3: Operating period i. Time evolution of: (a) influent and effluent nutrient concentration (NH_4^+, NO_2^-, NO_3^- and PO_4^{3-}); and (b) biomass concentration, total cells, solar irradiance (PAR) and temperature. The vertical line indicates the shift from sub-period i1 to sub-period i2.

Figure 4: Operating period ii. Time evolution of: (a) influent and effluent nutrient concentration (NH_4^+, NO_2^-, NO_3^- and PO_4^{3-}); and (b) biomass concentration, total cells, solar irradiance (PAR) and temperature.

Figure 5: Operating period iii. Time evolution of: (a) influent and effluent nutrient concentration (NH_4^+, NO_2^-, NO_3^- and PO_4^{3-}); and (b) biomass concentration, total cells, solar irradiance (PAR) and temperature. The vertical line indicates the shift from sub-period iii1 to sub-period iii2.

Figure 6: Operating period iii. Time evolution of: (a) nitrogen- and phosphorus-NRR (N-NRR and P-NRR, respectively), solar irradiance (PAR) and temperature; and (b) biomass concentration, solar irradiance (PAR) and temperature. The vertical line indicates the shift from sub-period iii1 to sub-period iii2.

TABLES

608 **Table 1:** Average operating and environmental conditions within the pseudo-steady state of each

609 operating (sub-)period.

Period	Duration (d)	HRT (days)	Allylthiourea $(mg \cdot L^{-1})$	Ammonium loading rate $(g\ NH_4\text{-}N \cdot d^{-1})$	Phosphate loading rate $(g\ PO_4\text{-}P \cdot d^{-1})$	Influent N:P ratio $(g\ N \cdot g^{-1}\ P)$	Solar irradiance $(\mu E \cdot m^{-2} \cdot s^{-1})$	Temperature (ºC)
P. i1	30	8	5	3.07 ± 0.07	0.36 ± 0.03	8.6 ± 0.9	148 ± 36	24.6 ± 0.6
P. i2	64	14	10	3.20 ± 0.73	0.36 ± 0.08	8.7 ± 0.4	124 ± 117	15.4 ± 0.8
P. ii	27	8	10	2.86 ± 0.09	0.37 ± 0.03	7.5 ± 0.6	317 ± 107	22.9 ± 2.1
P. iii1	24	8	10	2.61 ± 0.21	0.34 ± 0.02	7.7 ± 0.2	402 ± 84	20.7 ± 0.5
P. iii2	41			5.00 ± 0.46	0.58 ± 0.06	8.7 ± 0.5	290 ± 162	17.6 ± 2.2

610

611

612   Table 2: NRR, nutrient removal efficiency and biomass productivity within the pseudo-steady state of

613   each operating (sub-)period.

Period	Ammonium removal rate (mg N·L^{-1}·d^{-1})	Ammonium removal efficiency (%)	Phosphate removal rate (mg P·L^{-1}·d^{-1})	Phosphate removal efficiency (%)	Biomass productivity (mg VSS·L^{-1}·d^{-1})
P. i1	2.08 ± 1.17	41.6 ± 4.0	0.17 ± 0.17	36.1 ± 5.9	23.4 ± 0.6
P. i2	0.81 ± 0.52	50.9 ± 12.8	0.2 ± 0.01	50.9 ± 7.8	13.8 ± 1.1
P. ii	3.94 ± 0.35	54.4 ± 4.0	0.41 ± 0.07	55.9 ± 0.9	30.5 ± 1.8
P. iii1	4.75 ± 0.03	75.2 ± 2.2	0.51 ± 0.08	77.9 ± 1.4	41.0 ± 2.0
P. iii2	3.35 ± 0.57	36.3 ± 6.5	0.61 ± 0.13	45.5 ± 5.3	33.9 ± 3.1

614

615
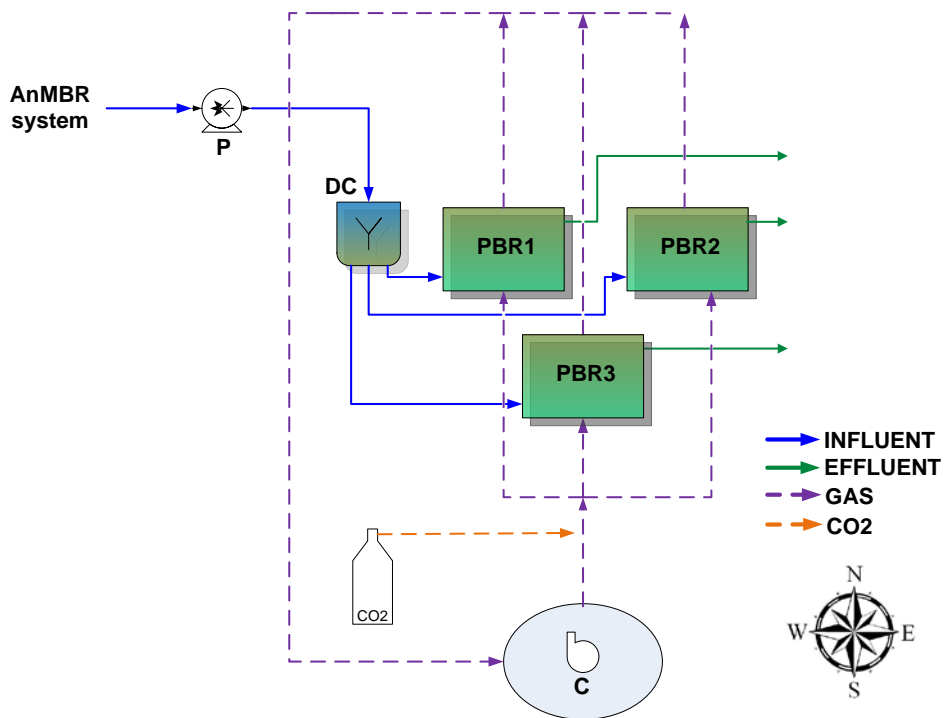
617   **Figure 1:** Flow diagram of the PBR system. Nomenclature: DC: distribution chamber; PBR:

618   photobioreactor; P: pump; C: compressor.

619
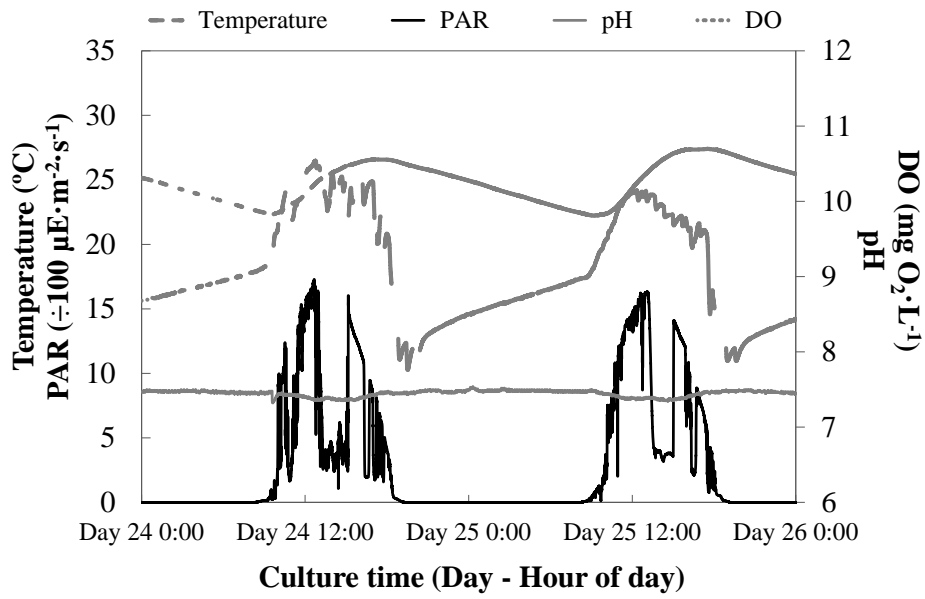
620

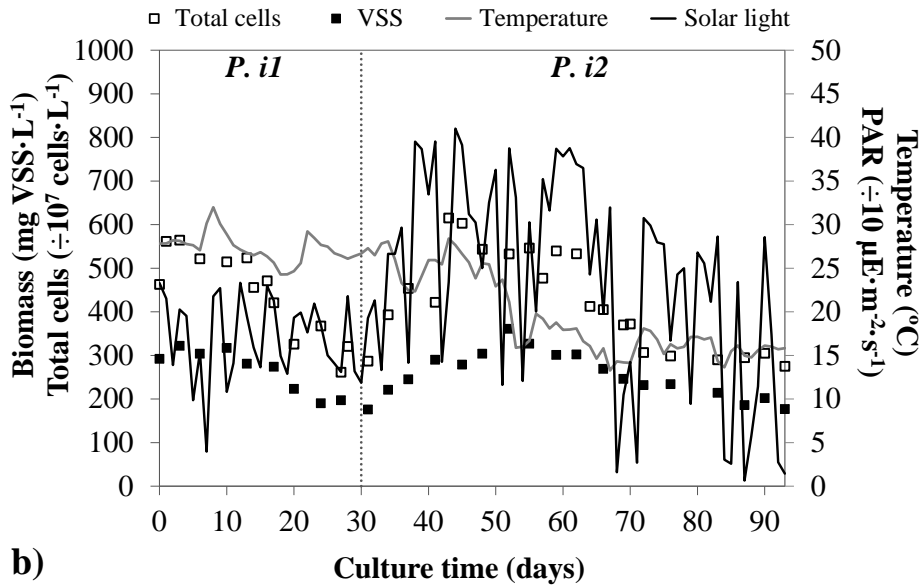**Figure 2:** Time evolution profiles within two days of operation of solar irradiance (PAR), temperature,
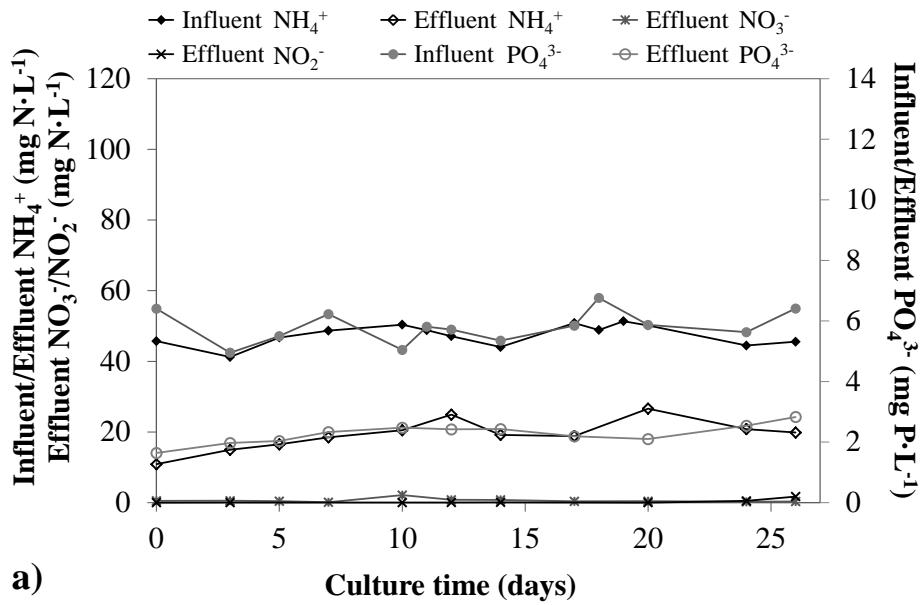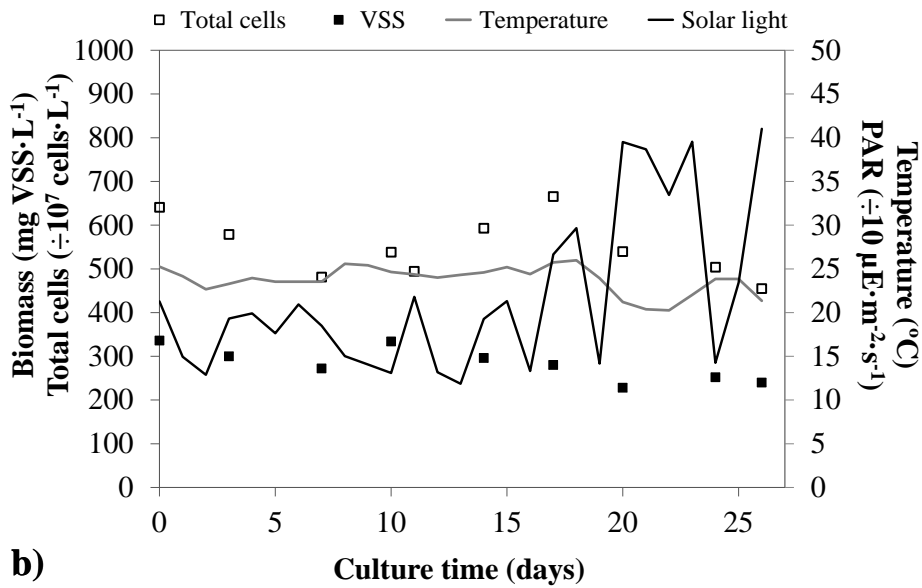
622   pH and DO.

623
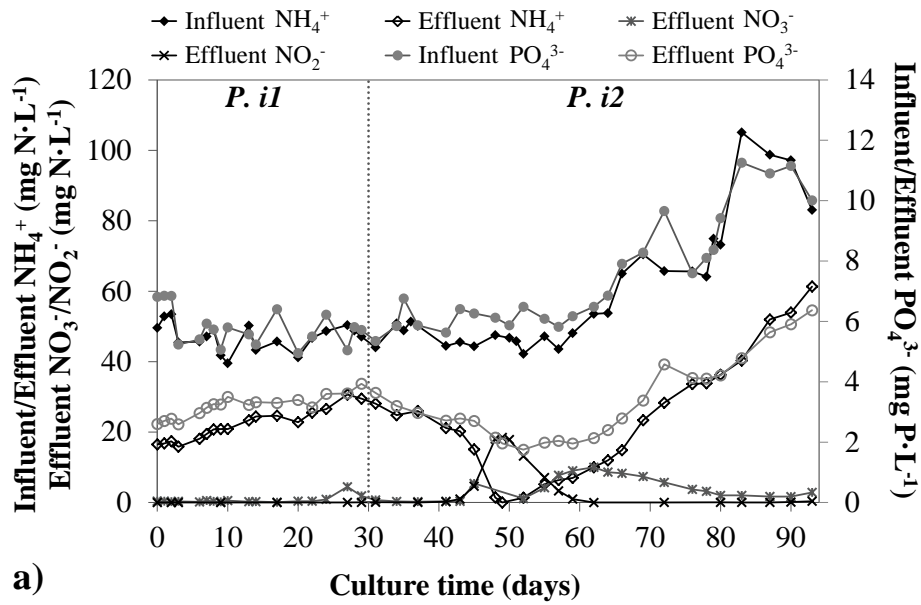
624   **a)**

625   **b)**
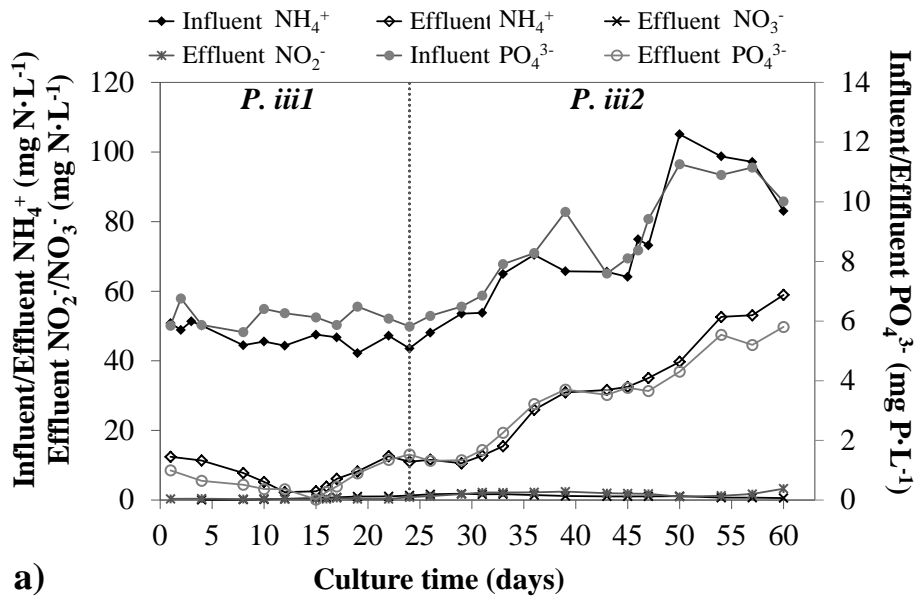
626   **Figure 3:** Operating period i. Time evolution of: (a) influent and effluent nutrient concentration (NH_4^+,

627   NO_2^-, NO_3^- and PO_4^{3-}); and (b) biomass concentration, total cells, solar irradiance (PAR) and temperature.

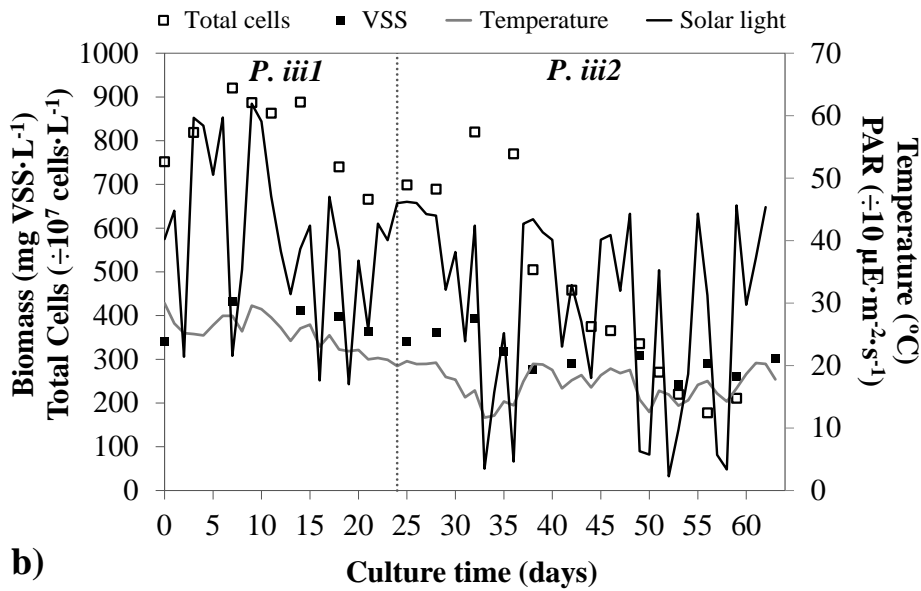628   The vertical line indicates the shift from sub-period i1 to sub-period i2.

629

630

a)

631

b)

632 **Figure 4:** Operating period ii. Time evolution of: (a) influent and effluent nutrient concentration (NH_4^+,

633 NO_2^-, NO_3^- and PO_4^{3-}); and (b) biomass concentration, total cells, solar irradiance (PAR) and temperature.
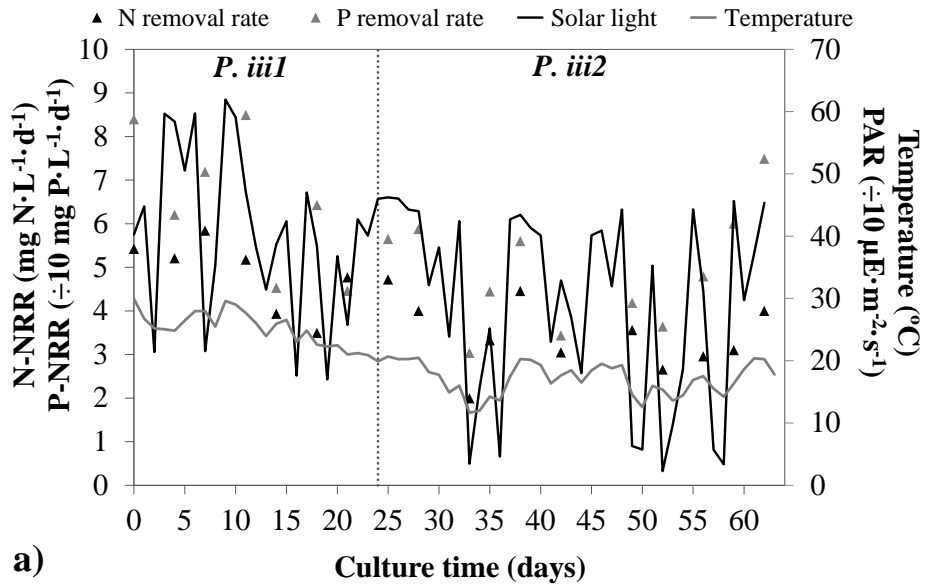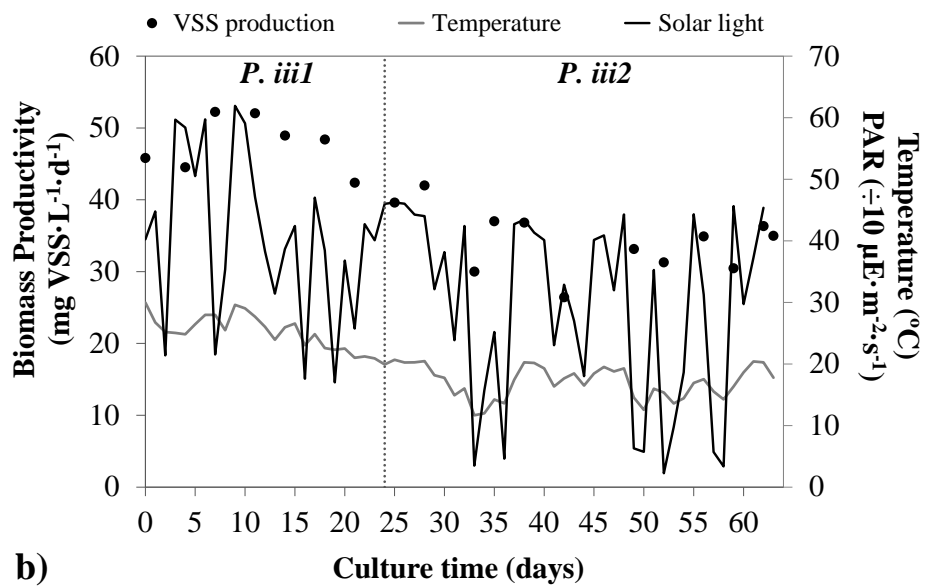
634

635   **a)**

636   **b)**

637   **Figure 5:** Operating period iii. Time evolution of: (a) influent and effluent nutrient concentration (NH_4^+,

638   NO_2^-, NO_3^- and PO_4^{3-}); and (b) biomass concentration, total cells, solar irradiance (PAR) and temperature.

639   The vertical line indicates the shift from sub-period iii1 to sub-period iii2.

640

641

642

Figure 6: Operating period iii. Time evolution of: (a) nitrogen- and phosphorus-NRR (N-NRR and P-NRR, respectively), solar irradiance (PAR) and temperature; and (b) biomass concentration, solar irradiance (PAR) and temperature. The vertical line indicates the shift from sub-period iii1 to sub-period iii2.

643

644

645

646

647